FI SEVIER

Contents lists available at ScienceDirect

## **Surface & Coatings Technology**

journal homepage: www.elsevier.com/locate/surfcoat



# The role of active species in the N<sub>2</sub> and N<sub>2</sub>-H<sub>2</sub> RF afterglows on selective surface nitriding of ALD-grown TiO<sub>2</sub> films



Yunfei Wang <sup>a</sup>, Andre Ricard <sup>b,\*</sup>, Jean-Philippe Sarrette <sup>b</sup>, Ansoon Kim <sup>c</sup>, Yu Kwon Kim <sup>a,\*</sup>

- <sup>a</sup> Department of Chemistry and Department of Energy Systems Research, Ajou University, Suwon 16499, South Korea
- b Université de Toulouse; UPS, INP; LAPLACE (Laboratoire Plasma et Conversion d'Energie), 118 route de Narbonne, F-31062 Toulouse, France
- <sup>c</sup> Korea Research Institute of Standards and Science (KRISS), Gajeongro 267, Yuseong-gu, Daejeon 34113, South Korea

#### ARTICLE INFO

Article history: Received 8 March 2017 Revised 29 April 2017 Accepted in revised form 29 May 2017 Available online 30 May 2017

Keywords: Active species N<sub>2</sub> afterglows N<sub>2</sub>-H<sub>2</sub> afterglows TiO<sub>2</sub> Surface nitriding

#### ABSTRACT

We find that surface modification characteristics of  $TiO_2$  using  $N_2$  RF plasma are strongly dependent on the detailed composition of active species in the plasma and the afterglows. The surface nitriding of ALD-grown  $TiO_2$  films in pure  $N_2$  RF afterglows at room temperature (RT) is found to be more effective in the late afterglows than in the early afterglows. Adding a small fraction of  $H_2$  in  $N_2$  results in suppression of surface nitriding, suggesting that the change in the composition of the active species in the afterglows by  $H_2$  is the origin to the suppressed nitriding performance. Here, we present our analysis on the surface chemical composition after the plasma modification as well as the densities of excited species such as  $N_2$  and  $N_2$ ( $N_2$ ) metastable molecules and  $N_2^+$  ions in the afterglows of RF  $N_2$  and  $N_2$ – $H_2$  (<5%) at different positions along the downstream by emission spectroscopy. The early afterglow of  $N_2$  changes from a pink to a late afterglow where the  $N_2$  +  $N_2$  recombination is the dominant process with the introduction of  $N_2$ . The roles of active species such as  $N_2$ -atoms and  $N_2^+$  ions on  $TiO_2$  surface nitriding are found to oppose to each other. We find that  $N_2$  atoms enhance the surface nitriding, while  $N_2^+$  ions are likely to deplete the surface-bound  $N_2$  species.

© 2017 Published by Elsevier B.V.

#### 1. Introduction

The fascinating photo-responsive properties of  $TiO_2$  in driving number of photocatalytic reactions [1,2] as well as the huge potential of engineering their electronic structure [3] and morphology [4–6] have led to intense research activities on  $TiO_2$  as can be found from huge publications on  $TiO_2$  in diverse applications such as water splitting [7], sensors [8], solar cells [9] and photocatalytic remediation [3].

The basic principle underlying such diverse applications of  $TiO_2$  is based on the photoexcitation of electrons from valence band (VB) to conduction band (CB) to produce excitons and their subsequent dynamics within the lattice [10,11]. For a high efficiency in photocatalytic or photovoltaic applications, the separation of those excitons, diffusion and reactions at the surface need to be achieved in a favorable way [2, 11]. In this regard, the surface modification of  $TiO_2$  has the utmost influence on the ultimate performance of  $TiO_2$  in such applications since all catalytic reactions take place at the interface between the catalyst and the reactants either in liquid or in gas phases [4,12–14]. The presence of defects or impurities at the surface has a significant influence on

the overall efficiency in photocatalytic [15–17] or photoelectrochemical processes [18].

Among many different surface modification techniques, plasma treatments have been employed many times to turn out to be quite effective in enhancing the photoresponse of TiO $_2$  materials [12,13,15–19]. In this case, the role of plasma treatments is generally suggested to have a beneficial effect on the enhancement of absorption of visible light [13, 16,19]. However, the influence of plasma treatments on the material's chemical structure can be widely different from the formation of reduced phases (e.g., TiO $_2$  –  $_x$ ) [15] with oxygen vacancies [16,17] to the introduction of nitride phases [12,19]. In this regard, the information on the type of active species in plasma responsible for the formation of new structures in the oxide materials would be valuable in engineering the material's property in a more controlled manner.

The promotional effect of plasma treatment on the material's catalytic properties may be further enhanced by optimizing the right condition for the surface treatment. For such a purpose, analysis on the active species in the plasmas and afterglows would provide a valuable information in determining the right condition. With this motivation in mind, we performed a systematic analysis on the active species in the  $N_2$  and  $N_2$ - $H_2$  flowing RF afterglows by emission spectroscopy and the resulting surface nitriding characteristics of TiO<sub>2</sub> films in the afterglows were analyzed by X-ray photoelectron spectroscopy (XPS).

<sup>\*</sup> Corresponding authors. *E-mail addresses*: ricard@laplace.univ-tlse.fr (A. Ricard), yukwonkim@ajou.ac.kr (Y.K. Kim).

 $N_2$  and  $N_2-H_2$  flowing microwave and RF afterglows studied by emission spectroscopy [20–22] are generally understood to have various kinds of active species such as the N atoms, the  $N_2(X,\nu)$  vibrational excited ground state, the  $N_2(A,a')$  metastable molecules and the  $N_2^+$  ions, which are determined by the result of complicated kinetic reactions in early and late afterglows [23–25]. The density of N-atoms, O-atoms in impurity,  $N_2(X,\nu>13)$  and  $N_2(A)$  metastable molecules and  $N_2^+$  ions in the afterglows have been quantitatively measured in RF (13.6 MHz) flowing afterglows by NO titration for N atoms and bandratio intensities for O atoms,  $N_2(A)$  and  $N_2(X,\nu>13)$  metastable molecules and  $N_2^+$  ions. Interesting finding in relation to changes in the active species density in  $N_2$ -H $_2$  afterglows is that the early afterglow changed from a pink (characterized by a strong emission of  $N_2^+$  ions) to a late afterglow (where the N atoms are dominant without  $N_2^+$  ions) by introducing a small amount  $(10^{-5}$ - $10^{-3})$  of  $H_2$  into  $N_2$  [21].

In this report, we present our analysis on the densities of N-atoms, O-atoms in impurity,  $N_2(X, \nu > 13)$  and  $N_2(A)$  metastable molecules and  $N_2^+$  ions in the  $N_2$  and  $N_2-H_2$  (<5%) early and late RF afterglows and their influences on the surface nitriding characteristics of the TiO<sub>2</sub> films. Since the treatment condition only allows the chemical changes at the skin-depth layer at the surface, we find a strong correlation between the densities of active species in the afterglows and the surface N content determined by the XPS analysis.

#### 2. Experimental details

The experimental set-up of the RF plasmas and afterglows is reproduced in Fig. 1 [26]. An afterglow quartz tube of 21 mm (I.D.) is connected to a discharge tube of 6 mm (I.D.). The RF plasma is produced between two rings separated by 2 cm in the discharge tube.

Fig. 1(a) shows typical discharge characteristics of RF plasmas of pure  $N_2$  and  $N_2 + H_2$  as well as their afterglows. At the operating condition of  $N_2$  flow rate of 1 slm, the pressure of 8 Torr and the applied power of 100 W, one can observe an afterglow starting at around z=22 cm after the capacitive RF discharge between the two Cu strips in the discharge tube. An early afterglow at the beginning extends along the 21 mm dia. Quartz tube up to about 15 cm long downstream and then a late afterglow appears starting at z=48 cm. The plasmas and the afterglows produce characteristic emissions originated from the neutral and ionized excited species of  $N_2$ , which can be measured by the optical emission spectra. The emission spectroscopy is performed by means of an optical fiber connected to a Monera 500 spectrometer

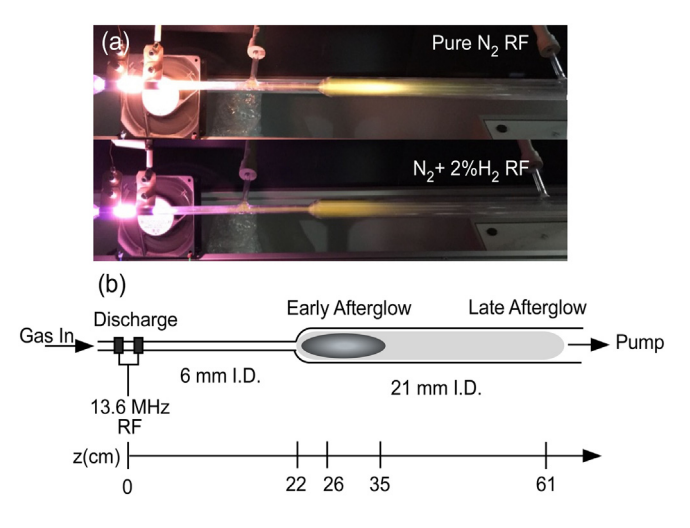


**Fig. 1.** (a) Pictures of our experimental setup for the generation of RF plasmas of  $N_2$  and  $N_2 + H_2$  as well as their afterglows under operating conditions and (b) a schematic diagram of our setup. The position of the measurement along the tube (z) is labelled with respect to the starting point (z=0) of the RF plasma generation.

with 500 mm focal length, grating blazed at 500 nm, slits of 0.5 mm, resolution of 0.8 nm and a PMT (Hamamatsu R928 at 900 V).

Fig. 1(a) also shows the picture of  $N_2$ -H<sub>2</sub> RF plasma and its afterglows. Here, we find that the emission intensity in the afterglow region is dramatically reduced compared to that of  $N_2$  afterglow as has been observed earlier [21]; the early (pink) afterglow changes to a late afterglow at z=26 cm with the  $N_2$ -H<sub>2</sub> mixture.

For the evaluation of plasma nitriding characteristics,  $TiO_2$  films were grown on a HF-cleaned Si substrate ((111), p-type, LG Siltron) by atomic-layer deposition (ALD) cycles (250 cycles) of titanium tetraisopropoxide (TTIP) and  $H_2O$  at the substrate temperature of 220 °C and the resulting film thickness is measured to be about 50 nm. The bulk phase of the ALD-grown  $TiO_2$  films is determined to be anatase from X-ray diffraction (XRD) measurements.

For the surface treatment of the  $TiO_2$  films in the afterglows, the sample was introduced into the 21 mm quartz tube at z=26 cm (the pink afterglow of the  $N_2$  RF plasma) and 61 cm (the late afterglow of the  $N_2$  RF plasma), respectively. For the  $N_2$ -H<sub>2</sub> case, the treatment position of 26 cm is selected since the position offers a high density of N atoms (~10<sup>15</sup> cm<sup>-3</sup>) in late afterglow conditions.

The X-ray photoelectron spectroscopy (XPS) measurements were performed in a PHI5000 Versa Probe II (Ulvac-PHI) system using a monochromatic Al K $\alpha$  source. The instrument work function is calibrated to the Au  $4f_{7/2}$  core level binding energy (BE) of 83.96 eV from a metallic gold film. The X-ray beam diameter can be set to  $200~\mu m$  and a charge neutralizer is used to minimize an undesirable charging effect. The binding energy for the spectra is referred by the C 1s peak from ubiquitous hydrocarbon to 284.8 eV.

#### 3. Results and discussion

#### 3.1. Pure $N_2$ pink and late afterglows

As shown in Fig. 2 the typical emission spectra of  $N_2$  are characterized by the  $N_2$  first positive (1st pos.) in the red part of spectrum between 500 and 1100 nm and by the  $N_2$  second positive (2nd pos.),  $N_2^+$  first negative (1st neg.) in the UV-blue part between 300 and 400 nm [21,26,27]. The characteristic  $N_2$  emissions are the 1st pos. (580 nm), 2nd pos. (316 nm) and  $N_2^+$ 1st neg. (391.4 nm) bands. The  $NO_\beta$  band at 320 nm is also detected in the  $N_2$  afterglow (Fig. 2(a)) coming from air impurity [27–29]. The NH (336 nm) emission is detected in  $N_2$ -H<sub>2</sub>(2%) as shown in Fig. 2(b).

After calibration of N atom density by NO titration [26], the density of N-atoms, O-atoms in impurity,  $N_2(X, \nu > 13)$  and  $N_2(A)$  metastable molecules and  $N_2^+$  ions are obtained by the line-ratio intensity method [27] and the results are reported in Table 1.

The  $a_{N+N}$  factor indicates the fraction of N+N recombination in the afterglow:  $a_{N+N}=0$  for pure pink (0%) and  $a_{N+N}=1$  for pure late (100%). Under the present operating condition of Table 1,  $a_{N+N}=1$  is measured to be 12% and 85% at z=35 and 61 cm, respectively.

The N-atom density calibrated by NO titration is obtained with an uncertainty of 30%. Only the order of magnitude of density is expected for the other active species:  $N_2(X, \nu > 13)$ ,  $N_2(A)$  and  $N_2^+$  which are depending on kinetic rates of the chosen dominant reactions.

To interpret the results in Table 1, it must be considered that the radial distribution of radiative states is sharp in the pink afterglow as reported in [21] at 8 Torr, 1 slm, 100 W,  $z=32\,\mathrm{cm}$ . The half-intensity width of the late afterglow is twice larger than that of the pink afterglow; that is, the pink afterglow has a narrower radial distribution in the tube than the late afterglow by a factor of a half. However, the estimated densities of active species from the emission data give only average values across the diameter of the tube since the emission intensity is the integrated emission along the line-of-sight. Thus, the densities at the center should be higher by a factor of two if the half-intensity width becomes narrower by half. Thus, the excited species densities in the pink afterglow reported in Table 1 at  $z=35\,\mathrm{cm}$  are multiplied by 2 to be

### Download English Version:

# https://daneshyari.com/en/article/5465081

Download Persian Version:

https://daneshyari.com/article/5465081

<u>Daneshyari.com</u>